Chapter 3

Influence of flexoelectricity on the EHD instabilities in nematics : a one-dimensional linear analysis for DC excitation

CHAPTER 3

INFLUENCE OF FLEXOELECTRICITY ON THE EHD INSTABILITIES IN NEMATICS: A ONE-DIMENSIONAL LINEAR ANALYSIS FOR DC EXCITATION

3.1 INTRODUCTION

It was shown by Meyer [1] that splay and bend distortions of the director field in a nematic can induce a macroscopic polarization in the medium. This property of a nematic is called flexoelectricity and is analogous to piezoelectricity in crystals. On the basis of the Meyer model only nematics made up of polar molecules having certain shapes can be expected to be strongly flexoelectric. It was later pointed out by Prost and Marcerou [2] that the electric quadrupole moments of the molecules also contribute to the flexoelectric effect, this contribution being independent of the molecular shape. Since nematogenic molecules generally have non-zero quadrupole moments, it follows that flexoelectricity is a universal property of all nematics.

The onset of an electrohydrodynamic (EHD) instability in a nematic, as discussed in the previous chapter, results in a periodic distortion of the director field. Such a distortion will give rise to a flexoelectric polarization $\vec{P}$ in the medium, given by [1]

$$\vec{P} = e_1 \hat{n} (div\hat{n}) + e_3 (curl\hat{n} \times \hat{n}) \qquad (1)$$

The action of the external electric field $\vec{E}$ on $\vec{P}$ will give rise to an additional torque on the director. Further, $\vec{P}$ will also contribute to the space charge density in the medium,

$$Q = div\vec{D} / 4\pi$$

where $\vec{D}$ is the displacement vector. These two flexoelectric contributions are not taken into account in the theories of EHD instabilities described earlier. In this chapter we first discuss the flexoelectric effect and then present an extension of the one-dimensional Helfrich model [3] for DC excitation incorporating flexoelectricity. These calculations show the importance of flexoelectricity in the formation of oblique rolls. Some experimental evidence is also presented in support of the theory.

3.2 FLEXOELECTRICITY

All the physical properties of nematics, discussed in chapter 1, indicate that the orientational ordering in the medium is apolar. However, as was shown by Meyer [1] in his original paper on flexoelectricity, a macroscopic polarization can be induced in a nematic by suitable deformations of the director field. According to the Meyer

model only nematics consisting of polar molecules having certain shapes can be strongly flexoelectric. For example, consider a nematic made up of pear shaped molecules with a non-zero longitudinal component of the electric dipole moment. In the undistorted state (Fig. 1a) because of the equal probability of both orientations, the dipole moments of the individual molecules cancel one another and the net dipole moment is zero. If the system is now splayed as in Fig. 1b, due to the pear shape, efficient packing of the molecules gives rise to a net dipole moment, resulting in a macroscopic polarization. A similar effect should be observed in a nematic made up of banana shaped molecules with a transverse electric dipole moment subjected to a bend distortion (Figs. 1c and 1d). For weak distortions the flexoelectric polarization is given by Eq.(1). We note here that this expression is the most general polar vector that can be constructed from the apolar director field $\hat{n}$, proportional to its first order derivatives. The flexoelectric coefficients e_1 and e_3 have the dimensions of charge / length. In the Meyer model e_1 arises in nematics made up of pear shaped molecules having a longitudinal dipole moment and e_3 in materials made up of banana shaped molecules having a transverse dipole moment. As mentioned earlier, Prost and Marcerou [2] pointed out that as the divergence of a quadrupole

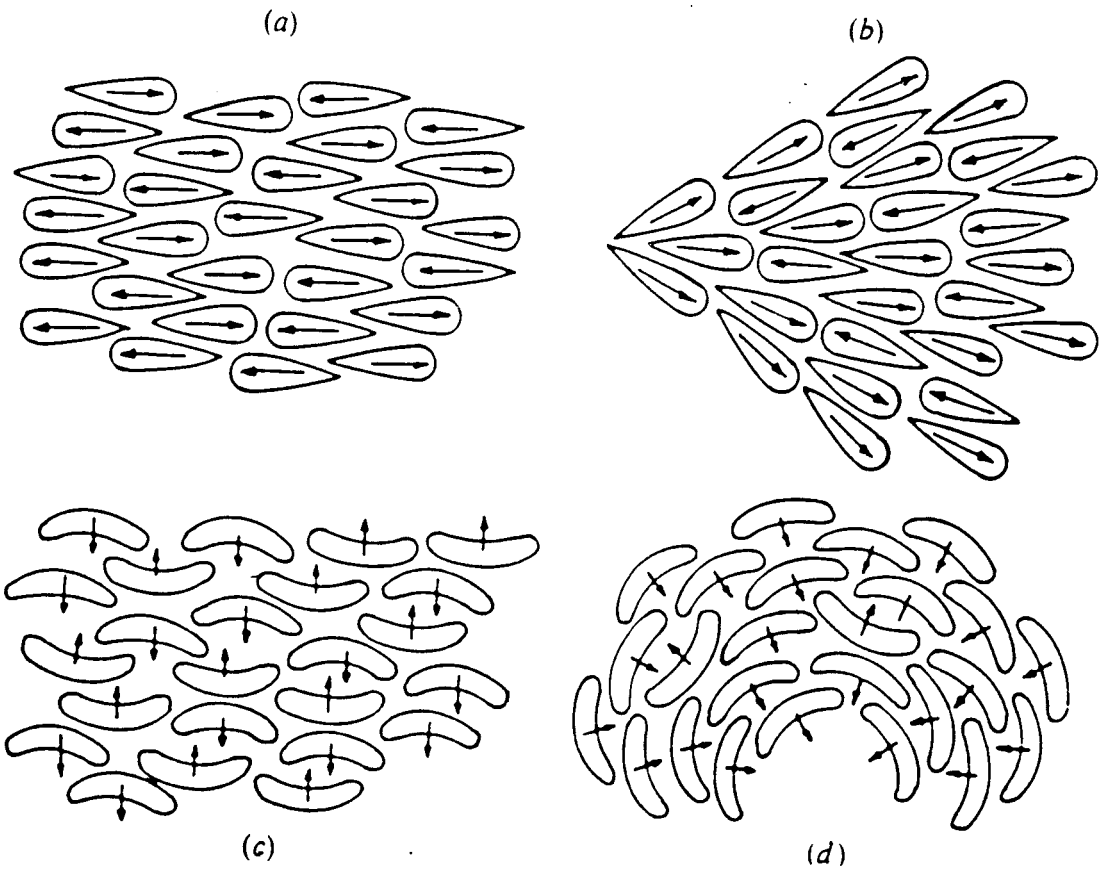

Fig.1. Origin of the flexoelectric effect according to the Meyer model [1]. A nematic consisting of pear shaped molecules with longitudinal dipole moment (a) becomes polarized under splay (b) and a nematic made up of banana shaped molecules with transverse dipole moment (c) becomes polarized under bend (d).

density is equivalent to a dipole density, there should be an additional contribution to the flexoelectric effect from the quadrupole moments of the molecules. This quadrupolar contribution is comparable in magnitude to the dipolar contribution discussed in the Meyer model, but unlike the latter contribution it is independent of the molecular shape. A11 nematogenic molecules generally have non-zero quadrupole moments. Therefore the theory of Prost and Marcerou leads to the important conclusion that flexoelectricity is a universal property of all nematics. In order to understand the origin of the quadrupolar contribution, let us consider a stacking of quadrupoles as shown in Fig.2. In Fig.2a, due to the symmetry of the arrangement, there is no net dipole moment in region *2.* If the structure is splayed, as can be seen from Fig.2b, the net dipole moment is non-zero in region *2,* and the structure becomes polarized.

The symmetry of a uniaxial phase allows non-zero electric quadrupole densities in the ground state, given by [2]

$$\Omega_{ij} = (1/u) \Sigma \theta^{n}_{ij} \quad ,$$

where the summation is performed over a suitable volume u and θ^{n}_{ij} is the quadrupole moment of the n^{th} molecule. It

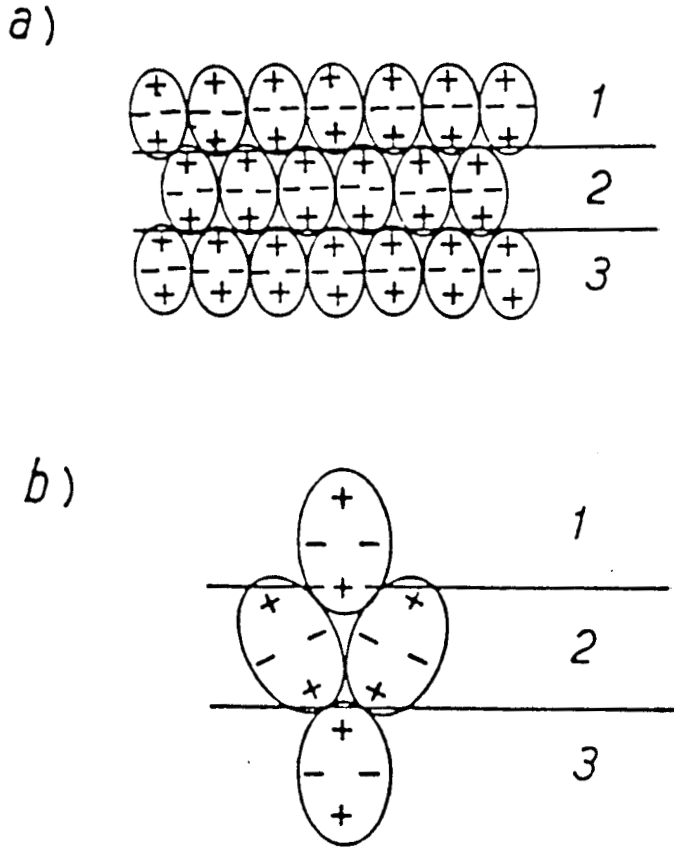

Fig.2. A regular stacking of quadrupoles (a). Because of the symmetry of the arrangement there is no bulk polarization. The structure becomes polarized when splayed (b).

is to be noted that though θ_{ij} is small ($\sim 10^{-25}$ esu) the density Ω_{ij} is not negligible since all the molecules in the volume. considered act cooperatively. Therefore,

$$\Omega_{ij} = N S \theta_a S_{ij} = \Omega_a S_{ij} ,$$

where N is the number of molecules per unit volume, θ_a the anisotropic part of the molecular quadrupole moment, S the orientational order parameter and $S_{ij} = (n_i n_j - \delta_{ij}/3)$. It was shown by Prost and Marcerou [2] that to a good approximation the quadrupolar contribution to the flexoelectric effect is given by

$$(e_1 + e_3) \approx -(2/3) \Omega_a .$$

In an electric field $\vec{E}$ the flexoelectric effect leads to a free energy density

$$f^{fl} = - \vec{P}.\vec{E}.$$

The corresponding molecular field obtained by minimizing f^{fl} is given by [4]

$$\vec{h}^{fl} = e_1 \{\vec{E} (div\hat{n}) - grad(\vec{E}.\hat{n})\} + e_3 \{ \vec{E} \times (curl\hat{n}) - curl(\vec{E} \times \hat{n})\} \quad (2)$$

The linear dependence of the flexoelectric energy on the curvature of the director field has some very interesting consequences. For example, if the distortion is planar described by a polar angle $\theta(z)$, say, then the flexoelectric energy identically satisfies the Euler-Lagrange equation

$$\delta f = (\partial f/\partial \theta) - \partial_z (\partial f/\partial \theta_{,z}) \quad ,$$

where $\partial_z = (\partial/\partial Z)$ and $\theta_{,z} = (\partial\theta/\partial Z)$, and therefore does not give rise to any volume torques in the medium. On the other hand, if the distortion is non-planar, described by two polar angles $\theta(z)$ and $\Phi(z)$, say, then $\mathbf{f}^{fL}$ does lead to volume torques. Hence we can expect an external electric field to induce a non-planar distortion in a nematic when the flexoelectric terms are dominant. Such flexoelectric distortions is the subject matter of chapter 6. In the case of the EHD instabilities we find that flexoelectricity can lead to a non-planar director distortion giving rise to oblique convective rolls.

3.3 THE ELECTROHYDRODYNAMIC EQUATIONS

Consider a homogeneously aligned nematic layer with the director $\hat{n}_o$ along the X-axis. Under the action of a DC electric field $\vec{E}_a$, applied along Z, we assume that

the EHD instability gives rise to oblique rolls whose wavevector $\vec{q}$ lies along ξ, making an angle a with $\hat{n}_o$ (Fig. 3). In the deformed state $\hat{n}$ makes polar angles θ and Φ in the XYZ system, so that the components of $\hat{n}$ in the $\xi\eta Z$ system are { $\cos\theta \cos(a-\Phi)$, $-\cos\theta \sin(a-\Phi)$, sine }. Since we are considering a one-dimensional model only the Z-component of the velocity appears in the equations describing the system. Further θ, Φ and v_z are functions of ξ alone. The transverse electric field created in the medium due to the space charge formation has by symmetry only the ξ-component E_ξ.

As mentioned earlier, the introduction of flexoelectricity can influence the problem in two ways. Firstly, the flexoelectric polarization contributes to the space charge density in the medium. Secondly, due to the flexoelectric coupling between the curvature of the director and the external electric field there is now an additional torque acting on the director. In order to clearly understand the influence of these two terms on the EHD instability we shall first consider a nematic with equal elastic constants and with $\epsilon_a = 0$.

Case I: $\epsilon_a = 0$, $K_1 = K_2 = K_3 = K$.

The system is described by the following equations

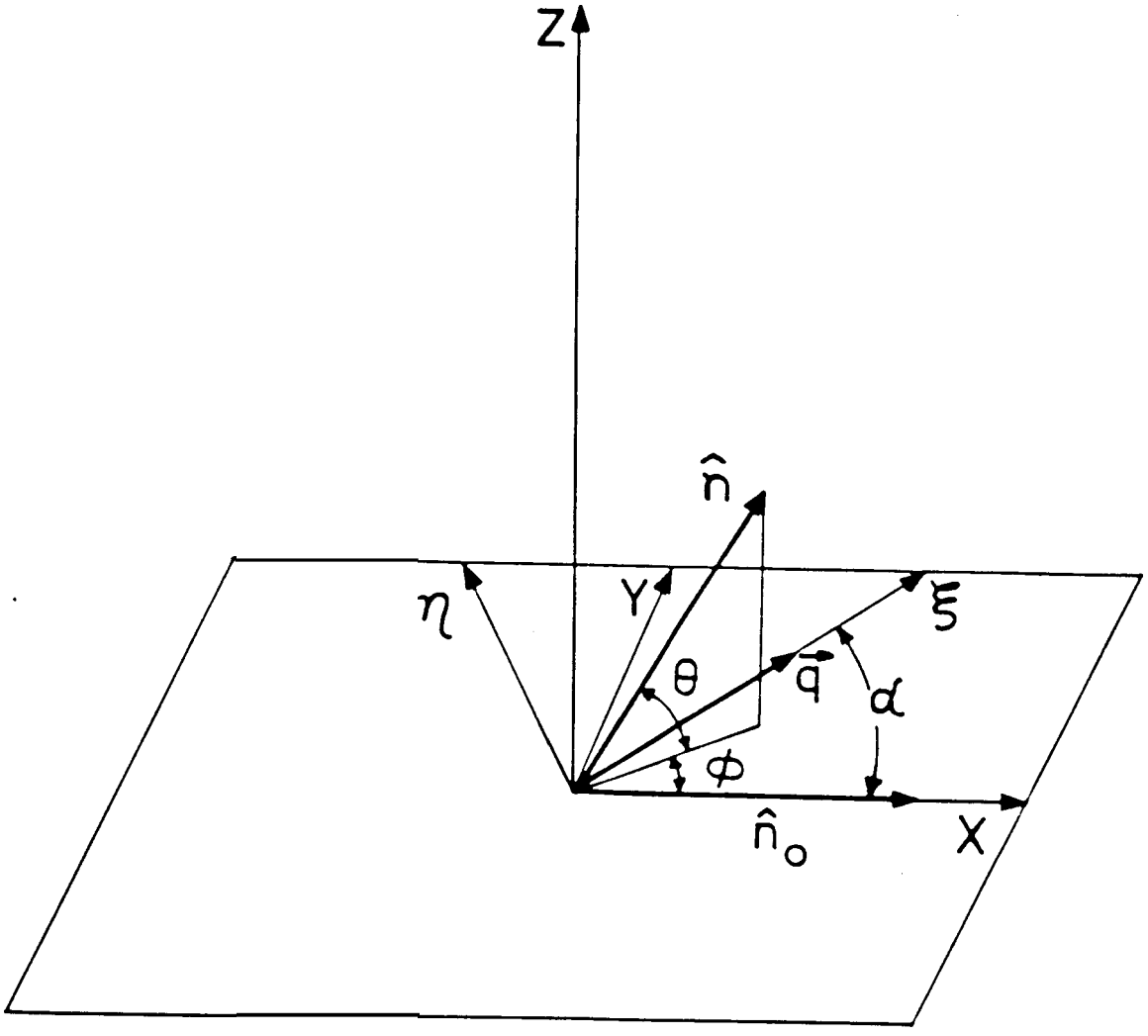

Fig.3. Illustration of the coordinate system and definitions of the angles used in the text.

1) The Poisson equation, div $\vec{D} = 4\pi Q$, where Q is the space charge density and the displacement vector $\vec{D}$ is given by

$$\vec{D} = \epsilon \vec{E} + 4\pi \vec{P},$$

where $\vec{P}$ is the flexoelectric polarization. Substituting these in the above equation, we get

$$\epsilon \left(dE_{\xi} / d\xi\right) + 4\pi \left(e_1 + e_3\right) s\, c \left(d^2\Phi/d\xi^2\right) = 4\pi Q \qquad (3)$$

where s = sin a and c = cos a.

2) The charge conservation equation,

$$\left(\partial Q/ \partial t\right) + \operatorname{div} \vec{J} = 0$$

Since we are considering only stationary solutions under DC excitation the time dependence of all variables can be neglected. Substituting the expression for the current density $\vec{J}$ (see Eq.(8), Chapter 1), the above equation reduces to

$$\sigma_c \left(dE_{\xi} / d\xi\right) + \sigma_a E_a c \left(d\theta/d\xi\right) = 0 \qquad (4)$$

where $\sigma_c = \sigma_{\perp} + \sigma_a c^2$.

3) The equation of motion [5]

$$\rho\left(\partial \vec{v}/ \partial t\right) + \operatorname{div} \left(\rho \vec{v}\vec{v}\right) = \operatorname{div} \left(\bar{\bar{\sigma}} + \bar{\bar{\sigma}}'\right) + Q\vec{E}$$

where ρ is the density, $\vec{\vec{a}}$ the elastic stress tensor and $\vec{\vec{a}}'$ the viscous stress tensor. In the one-dimensional model only the Z-component of the above equation exists. The time dependence can be neglected as we are looking for stationary solutions. Further, $\bar{a}$ does not lead to any linear terms. The equation of motion then reduces to

$$-\eta_1 (d^2 v_z / d\xi^2) = Q E_a \qquad (5)$$

where $\eta_1 = \frac{1}{2}[a_4 + (a_5 - a_2)c^2]$.

4) The torque balance equation,

$$\Gamma_i^d + \Gamma_i^{fl} = \Gamma_i^{hy} \quad , \quad i = Y, Z.$$

Here $\vec{\Gamma}^d$, $\vec{\Gamma}^{fl}$ and $\vec{\Gamma}^{hy}$ are the elastic, flexoelectric and the viscous torques, respectively. They can be obtained from the corresponding molecular fields using the relation $\vec{\Gamma} = \hat{n} \times \vec{h}$. The torque balance equation along Y yields

$$K(d^2\theta/d\xi^2) + (e_1 - e_3)E_a s(d\Phi/d\xi) - a_2 c(dv_z/d\xi) = 0 \qquad (6)$$

Similarly the torque balance equation along Z yields

$$K(d^2\Phi/d\xi^2) - (e_1 - e_3)E_a s(d\theta/d\xi) + (e_1 + e_3)E_a \sigma_r s c^2 (d\theta/d\xi) = 0 \qquad (7)$$

where $\sigma_r = \sigma_d/\sigma_c$.

Using Eqs.(3-5) v_z can be eliminated from Eq.(6) and we get

$$K(d^2\theta/d\xi^2) + [(e_1 - e_3) + (a_2/\eta_1)(e_1 + e_3)c^2]E_a s (d\Phi/d\xi) - (a_2 \epsilon/4\pi\eta_1)\sigma_r E_a^2 c^2 \theta = 0 \qquad (8)$$

The system is described by the two coupled equations (7) and (8), which clearly admit the following solutions:

$$\theta = \theta_0 \sin q\xi \quad \text{and} \quad \Phi = \Phi_0 \cos q\xi$$

Substituting these solutions in the above equations the condition for the existence of non-trivial solutions gives the following relation between E_a and q.

$$E_a^2 = 4\pi q^2 K^2 / (-a_2 \epsilon K \sigma_r c^2 / \eta_1 + 4\pi F s^2) \qquad (9)$$

where

$$F = (e_1 - e_3)^2 - (e_1 + e_3)^2 \sigma_r a_2 c^4 / \eta_1 + (e_1 + e_3)(e_1 - e_3)(a_2/\eta_1 - \sigma_r) c^2$$

As in the Helfrich model we assume that $q = \pi/d$ at the threshold. Then we get a voltage threshold given by

$$V_{th}^2 = 4\pi^3 K^2 /(-a_2 \epsilon K \sigma_r c^2 / \eta_1 + 4\pi F s^2) \qquad (10)$$

For a given set of values of the material parameters the threshold voltage can be calculated for different values of the angle a. The lowest value of V_{th} gives the critical voltage V_c for the onset of the instability and the corresponding value of a gives the **tilt** of the convective rolls at the threshold. The variation of V_{th} calculated for $\epsilon_{\parallel} = \epsilon_{\perp} = 5.2$, $K_1 = K_2 = K_3 = 6.3 \times 10^{-7}$ dynes and the standard MBBA values of the other material parameters, listed in table 1, is shown in **Fig.4. It** is clear from the figure that the instability sets in at a critical voltage of about 1.7 Volts with a $\approx$ ***0.85*** radians. Thus the flexoelectric effect clearly leads to the formation of oblique rolls even in the context of a one-dimensional model.

Case II: $\epsilon_a \neq 0$, $K_1 \neq K_2 \neq K_3$.

The above analysis can be generalized to the case with non-zero dielectric and elastic anisotropies. **Eqs.**(7) and (8) now read

$$M(d^2\theta/d\xi^2) + [(e_1 - e_3) + (a_2/\eta_1)(e_1 + e_3) c^2]E_a s (d\Phi/d\xi)$$
$$+[\epsilon_a \sigma_{\perp} /(4\pi \sigma_c) + (\epsilon_r - \sigma_r) a_2 \epsilon_c c^2/(4\pi \eta_1)]E_a^2 \theta = 0 \qquad (11)$$

and,

TABLE 1

Material parameters of MBBA

K_1 = 6.1 x 10^{-7} dyne (a)	a_1 = 6.5 cP (c)
K_2 = 4.0 x 10^{-7} dyne (b)	α_2 = -77.5 cP (c)
K_3 = 7.3 x 10^{-7} dyne (a)	α_3 = -1.2 cP (c)
$\epsilon_{\parallel}$ = 4.7 (a)	α_4 = 83.2 cP (c)
$\epsilon_{\perp}$ = 5.2 (a)	α_5 = 46.3 cP (c)
$a_{\parallel}$ = 1.0 x 10^{-10} $ohm^{-1}cm^{-1}$	$\sigma_a/\sigma_{\perp}$ = 0.5 (a)
$(e_1 - e_3)$ = 1.2 x 10^{-4} cgs units (d)	
$(e_1 + e_3)$ = -7.0 x 10^{-4} cgs units (e)	

(a) P.A. Penz and G.W. Ford, Phys. Rev, **A6**, 414 (1972).

(b) L.M. Blinov, Electro-optical and Magneto-optical properties of Liquid Crystals, Wiley, 1983.

(c) P.G. de Gennes, The Physics of Liquid Crystals, Oxford, Clarendon, 1975.

(d) I. Dozov, Ph. Martinot-Lagarde and G. Durand, J. de Phys., **43**, L365 (1982).

(e) N.V. Madhusudana and G. Durand, J. de Phys., **46**, L195 (1985).

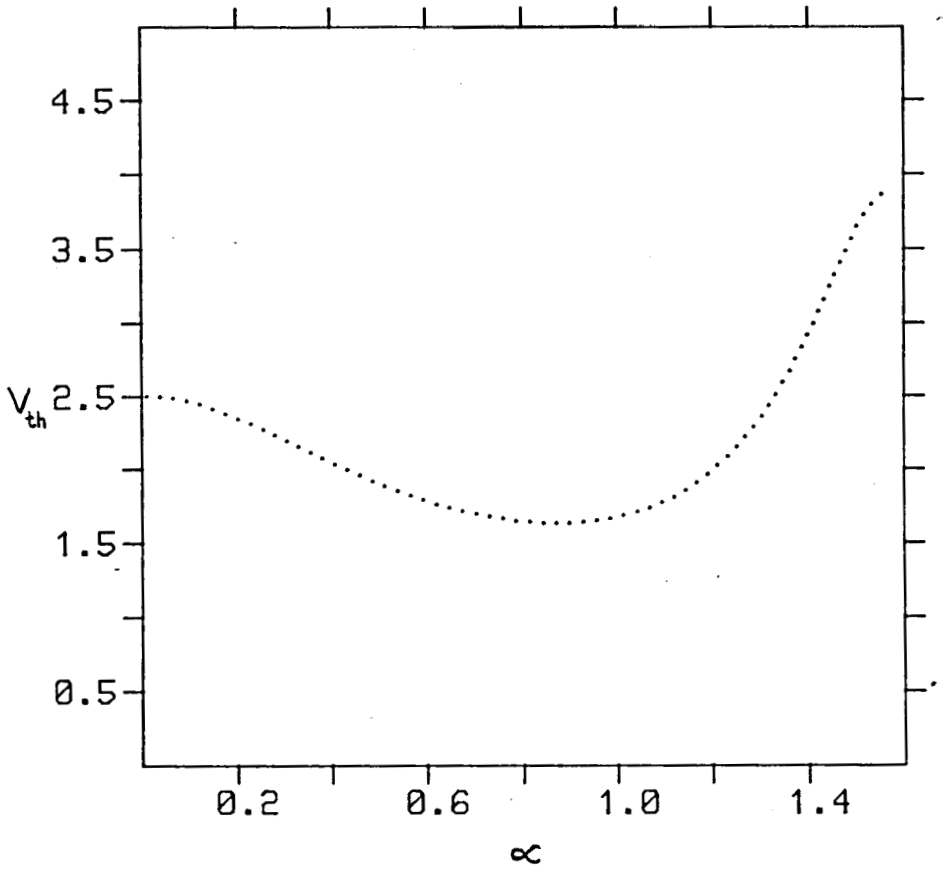

Fig.4. Variation of the threshold voltage V_{th} (in Volts) with a (in radians) calculated for $\epsilon_{\parallel} = \epsilon_{\perp} = 5.2$ and $K_1 = K_2 = K_3 = 6.3 \times 10^{-7}$ dynes and the standard MBBA values of the other material parameters.

$$L(d^2\Phi/d\xi^2) - (e - e_3)E_a s\,(d\theta/d\xi) + (e_1 + e_3)E_a\sigma_r S\,c^2(d\theta/d\xi) = 0 \qquad (12)$$

where $M = K_2 s^2 + K_3 c^2$, $L = K_1 s^4 + K_3 c^2$ and $\epsilon_r = \epsilon_a/\epsilon_c$. The threshold voltage is now given by

$$V_{th}^2 = ML\,\pi^2/[\{\epsilon_a\sigma_\perp/\sigma_c + (\epsilon_r - \sigma_r)a_2\epsilon_c c^2/\eta_1\}L/4\pi + F\,s^2] \qquad (13)$$

The variation of V_{th} with a calculated from Eq. (13) using the standard MBBA values of the parameters is shown in Fig.5. It is clear from the figure that the instability sets in at a critical voltage of about 1.75 Volts and with a ≈ 0.83 radians. When a $=0$, the flexoelectric terms vanish from Eq.(13) and it reduces to that given by Helfrich [3]. On the other hand, when a $=\pi/2$, all the hydrodynamic terms are absent and the flexoelectric effect can cause a static periodic distortion of the director field if ϵ_a is sufficiently small. These flexoelectric distortions are discussed in chapter 6.

3.4 RESULTS AND DISCUSSION

Eqs.(10) and (13) show that the flexoelectric terms are entirely responsible for the occurrence of oblique rolls in the context of a one-dimensional model. The dependence of a on the flexoelectric coefficients can be understood

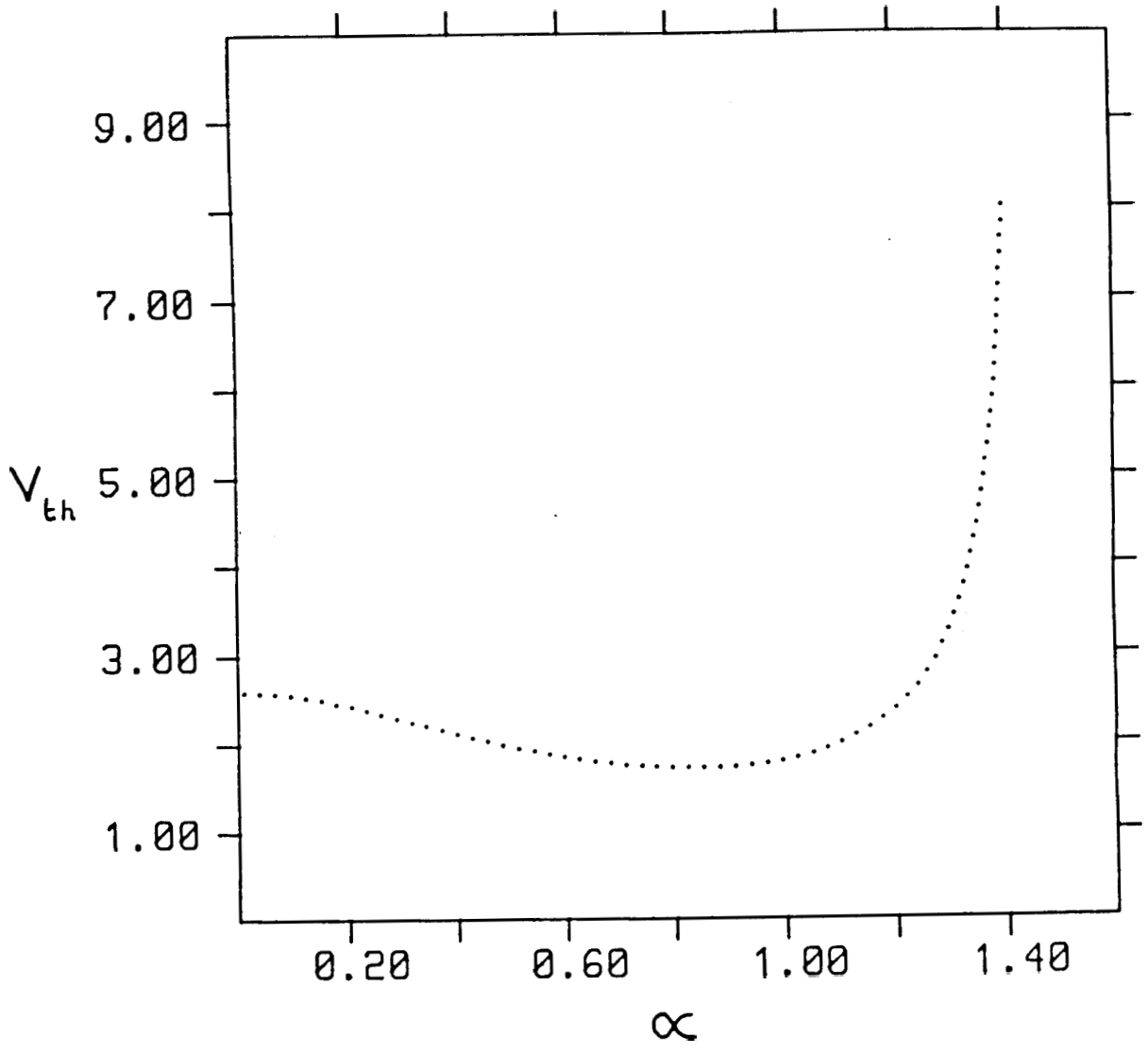

Fig.5. Variation of the threshold voltage V_{th} (in volts) with a (in radians) calculated for the standard MBBA values of the material parameters.

using the torque balance equations which are reproduced below. For the sake of simplicity we shall first consider the case with $\epsilon_a = 0$ and equal elastic constants.

$$K(d^2\Phi/d\xi^2) - (e_1 - e_3)E_a s(d\theta/d\xi) + (e_1 + e_3)E_a \sigma_r s\, c^2(d\theta/d\xi) = 0 \qquad (7)$$

$$K(d^2\theta/d\xi^2) + [(e_1 - e_3) + (e_1 + e_3)\, c^2 \alpha_2/\eta_1]E_a s\,(d\Phi/d\xi) - [\alpha_2 \epsilon\, \sigma_r/(4\pi\eta_1)]\, E_a^2 c^2 \theta = 0 \qquad (8)$$

We note here that only the combinations $(e_1 - e_3)$ and $(e_1 + e_3)$ of the flexoelectric coefficients appear in these equations. The $(e_1 - e_3)$ terms in the two equations give the torque arising from the action of. the external field on the curvature of the director field. The $(e_1 + e_3)$ term in Eq.(7) is the torque due to the gradient of the transverse electric field in the medium and the $(e_1 + e_3)$ in Eq.(8) the hydrodynamic torque due to the action of the external field on the space charge density arising from the flexoelectric polarization. If $(e_1 - e_3)$ and $(e_1 + e_3)$ have opposite signs then the two flexoelectric terms in Eq.(7) assist each other and favour a @-distortionof the director. Let us choose $(e_1 - e_3)$ and $(e_1 + e_3)$ to be positive and negative, respectively, as is found experimentally in MBBA. Taking θ_o, E_a and **a** to be positive we find

from Eq.(7) that Φ_o is negative. Since a, is generally negative, both the flexoelectric terms in Eq.(8) have the same sign. Further, the flexoelectric torques will be destabilizing if Φ_o is negative: at the threshold of the instability a @-distortion of the director and hence a non-zero value of a are favoured. Similar arguments apply when the signs of both θ_o and Φ_o are reversed.

The dependence of a on $(e_1 - e_3)$ is shown in Fig.6. As $(e_1 - e_3)$ is decreased from its initial positive value, the flexoelectric torques decrease and a decreases. As a becomes smaller the hydrodynamic torque becomes more dominant and the decrease in a becomes very rapid. When $(e_1 - e_3)$ is negative and approximately equal to $(e_1 + e_3)\sigma_a/\sigma_{11}$, the sum of the flexoelectric terms in Eq.(7) becomes negligible and a goes to zero. As $(e_1 - e_3)$ is decreased further the threshold for the static flexoelectric domains becomes smaller than that for the EHD instability when

$$|e_1 - e_3| > [-2a_2 \epsilon K \sigma_a /\{(a_4 + a_5 - a_2)\sigma_{11}\}]^{1/2}$$

and $a = \pi/2$. Thus for a very small range of negative values of $(e_1 - e_3)$, $a = 0$ and the flexoelectric terms do not influence the problem.

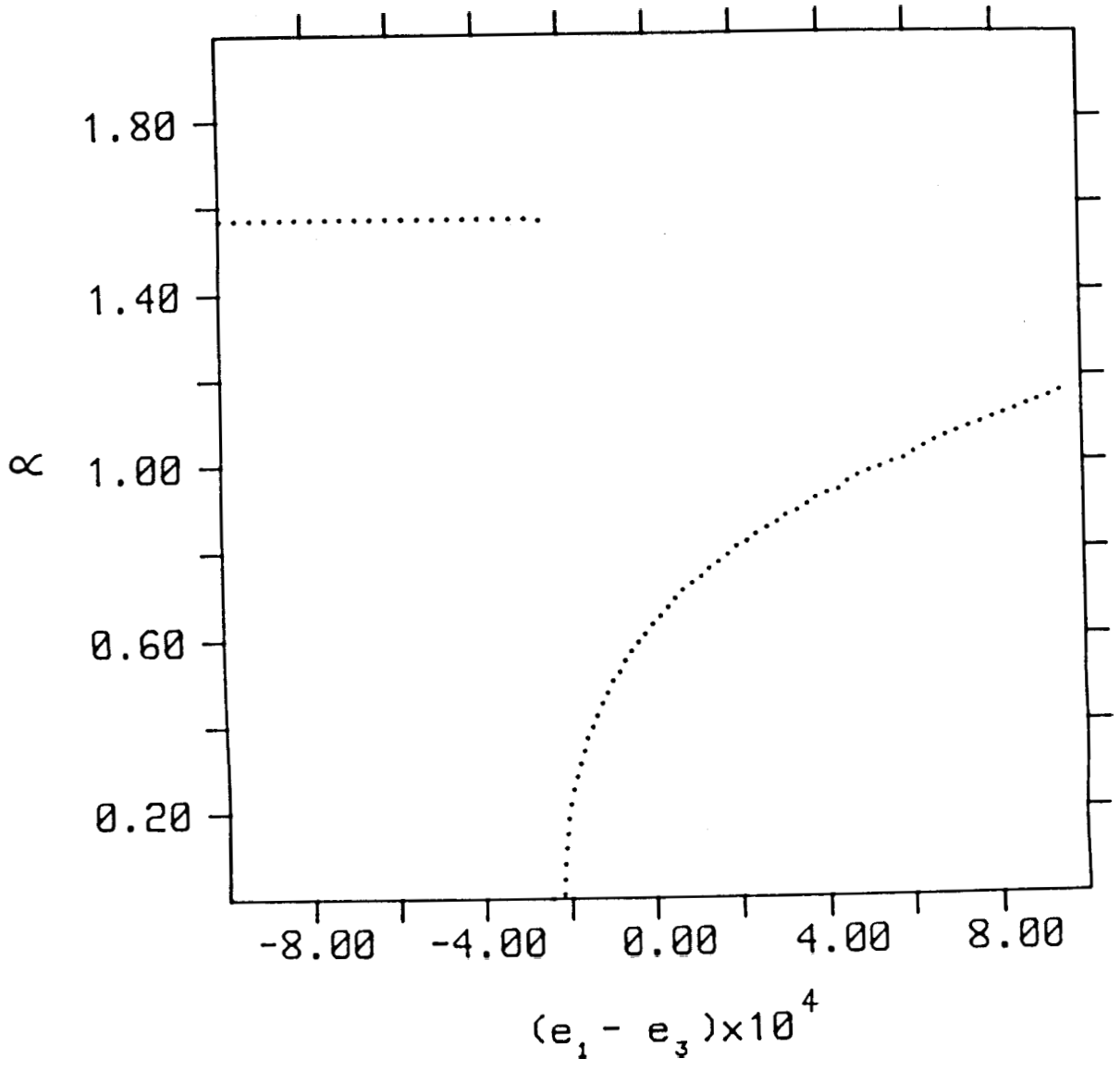

Fig.6. Variation of a (in radians) with $(e_1 - e_3)$ (in cgs units) calculated for $\epsilon_{\parallel} = \epsilon_{\perp} = 5.2$ and $K_1 = K_2 = K_3 = 6.3 \times 10^{-7}$ dynes. Note that a = 0 for a very small range of negative values of $(e_1 - e_3)$ and below this range the longitudinal flexoelectric domains are obtained.

The variation of a with $(e_1 + e_3)$ is shown in Fig.7. As $(e_1 + e_3)$ is increased from its initial negative value, the flexoelectric torques decrease and hence a decreases. When $(e_1 + e_3)$ is positive and in the range

$$-(e_1 - e_3)(a_4 + a_5 - a_2)/(2a_2) < (e_1 + e_3) < (e_1 - e_3)\sigma_{\parallel}/\sigma_a,$$

Eqs. (7) and (8) cannot be simultaneously satisfied by nonzero values of Φ. As seen from Fig.7, a =0 over a wider range because of the dominance of the hydrodynamic torque at small values of a.

If we now introduce the elastic anisotropy, Eqs. (11) and (12) show that as K_1 and K_2 are less than K_3 in MBBA, the elastic anisotropy favours a non-zero value of a. This is reflected in Figs. 8 and 9, which show the variation of a with $(e_1 - e_3)$ and $(e_1 + e_3)$, respectively, for $\epsilon_a = 0$ and $K_1 \neq K_2 \neq K_3$.

The variations of V_c and a with ϵ_a are shown in Figs.10 and 11. As ϵ_a is increased the stabilizing torque on the director decreases and V_c decreases. It should be noted that beyond a certain positive value of ϵ_a the Freedericksz transition has a lower threshold than the EHD instability. When ϵ_a is negative the space charge

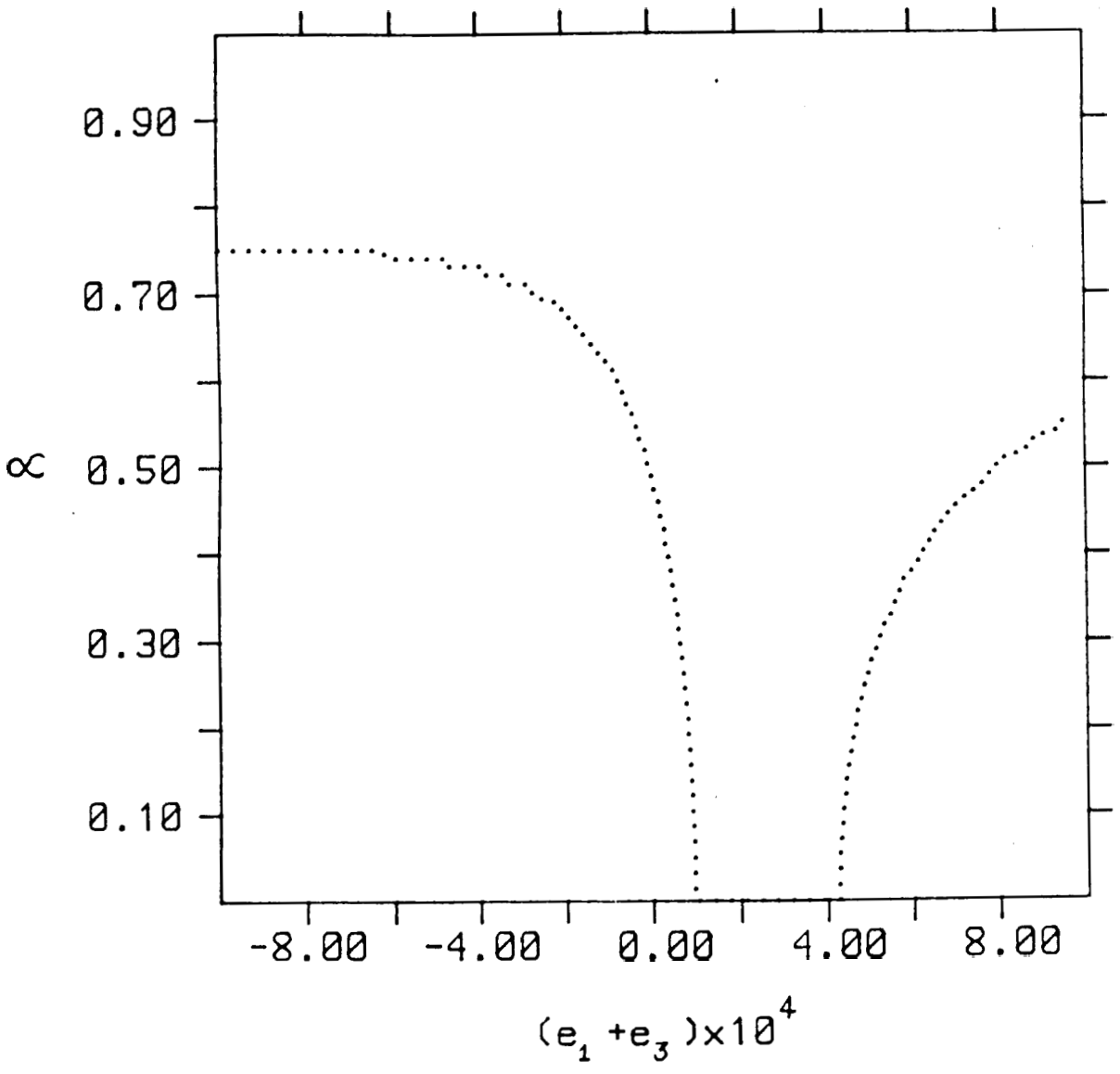

Fig.7. Variation of a (in radians) with $(e_1 + e_3)$ (in cgs units) calculated for $\epsilon_{\parallel} = \epsilon_{\perp} = 5.2$ and $K_1 = K_2 = K_3 = 6.3 \times 10^{-7}$ dynes. Note that a = 0 for a small range of positive values of $(e_1 + e_3)$.

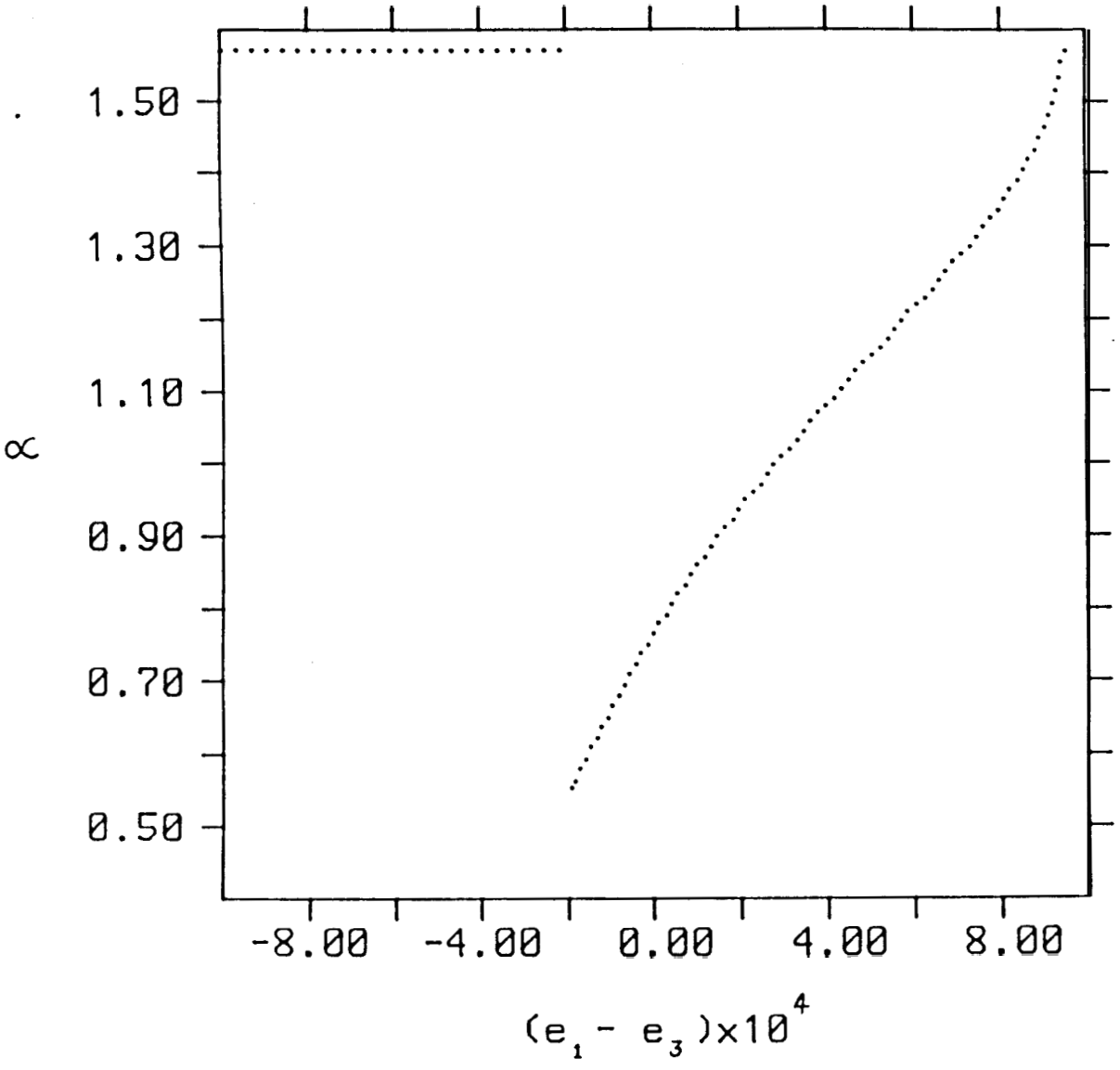

Fig.8. Variation of a (in radians) with $(e_1 - e_3)$ (in cgs units) calculated for $\epsilon_{\parallel} = \epsilon_{\perp} = 5.2$ and including the elastic anisotropy. Note that a does not go to zero in this case.

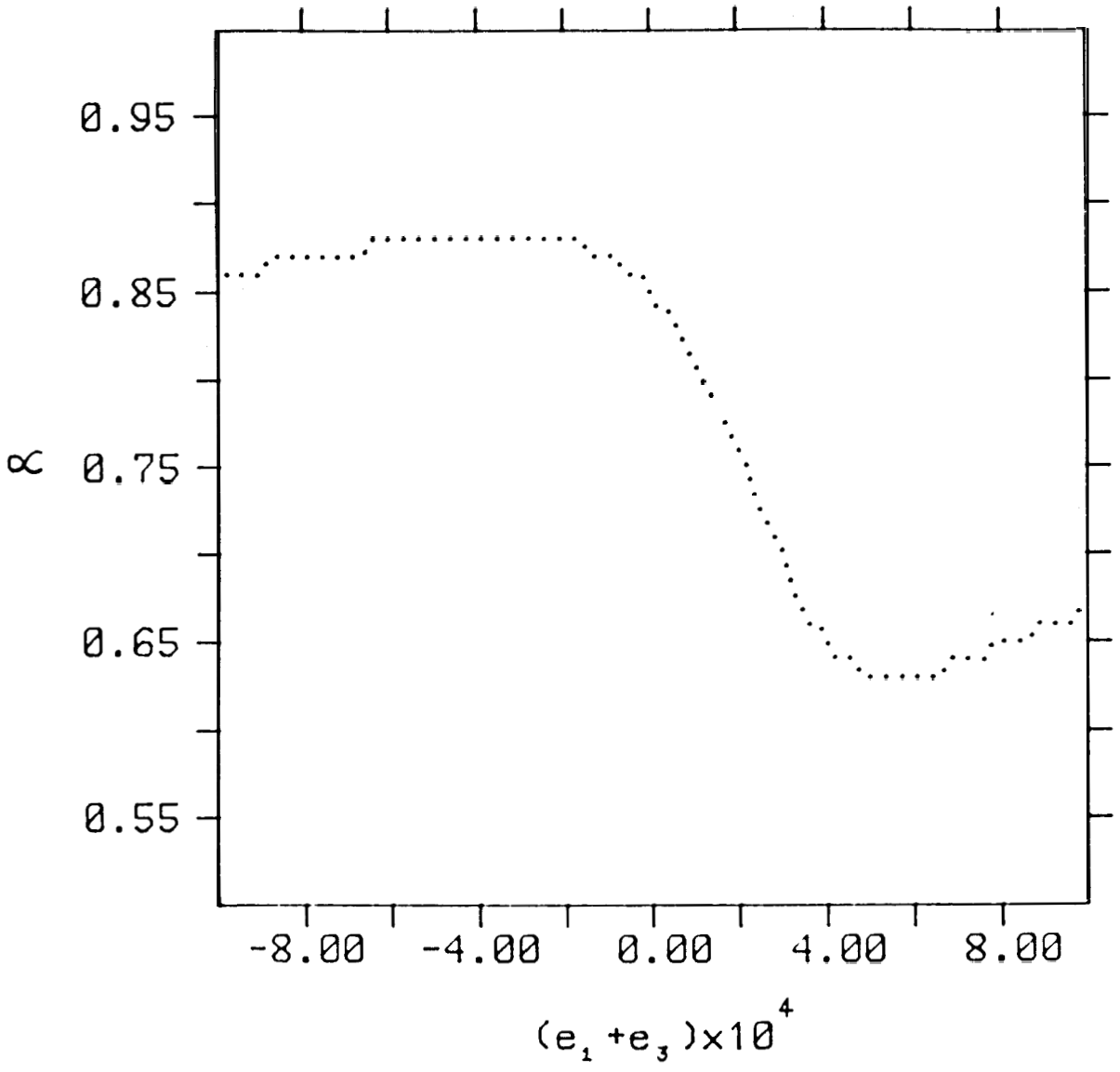

Fig.9. Variation of a (in radians) with $(e_1 + e_3)$ (in cgs units) calculated for $\epsilon_{\parallel} = \epsilon_{\perp} = 5.2$ and including the elastic anisotropy. Note that a does not go to zero in this case. In this and a few other figures to follow, the courseness in the plot is due to a relatively low resolution on the monitor from which a hard copy was obtained.

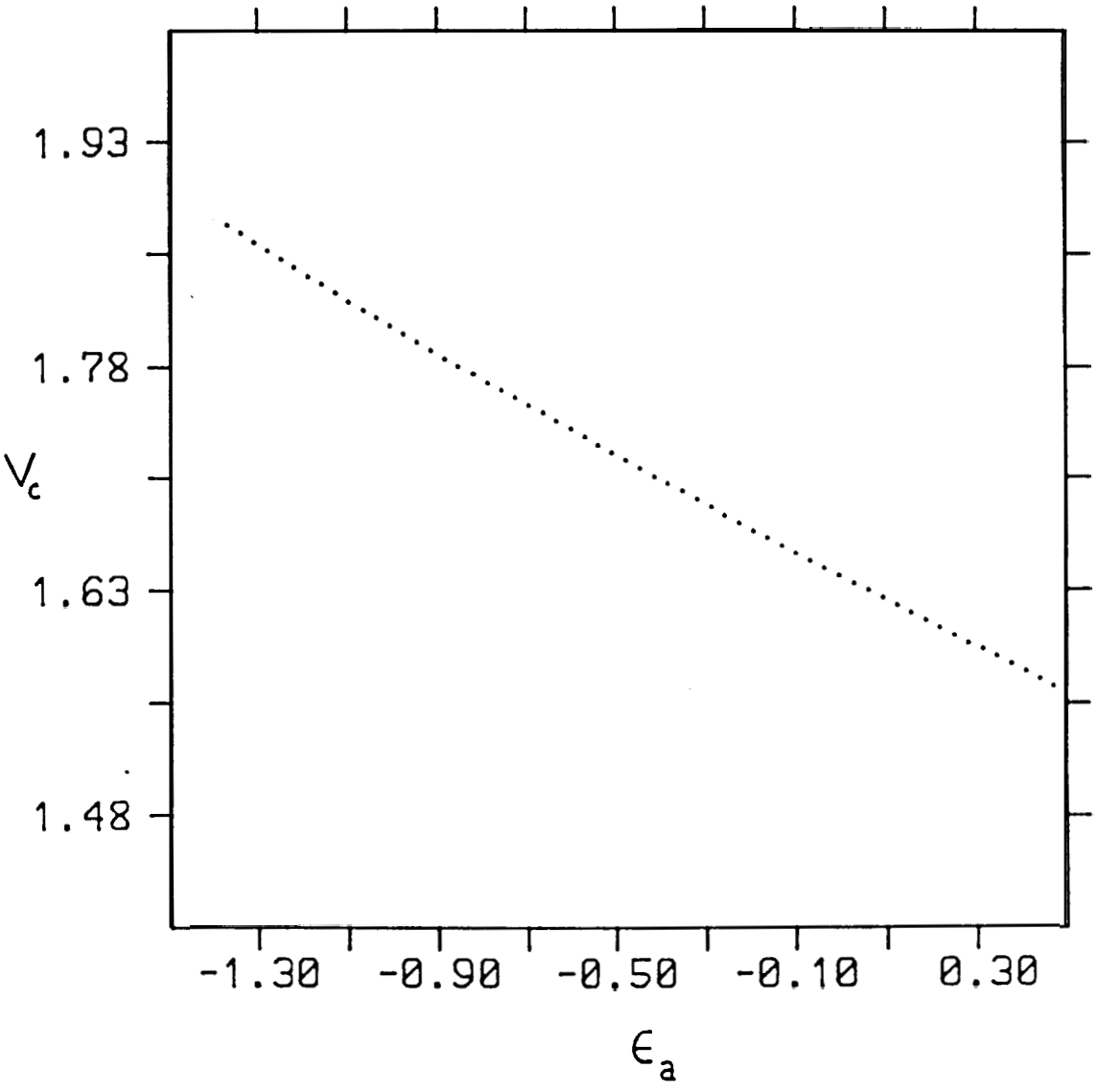

Fig.10. Variation of the critical voltage V_c (in Volts) with the dielectric anisotropy ϵ_a.

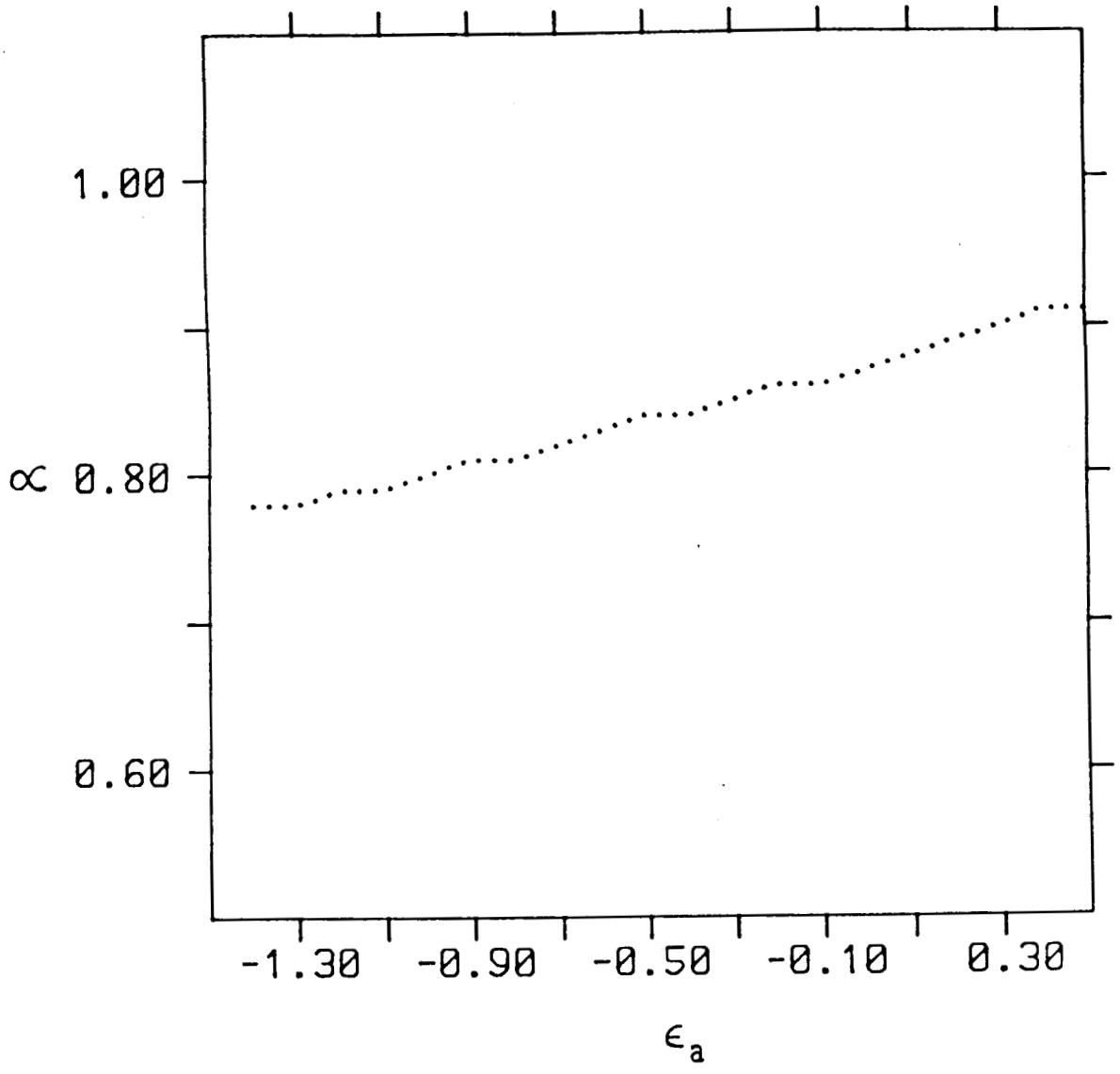

Fig.11. Variation of a (in radians) with the dielectric anisotropy ϵ_a.

density due to the dielectric polarization has the same sign as that due to the conductivity anisotropy. Therefore, on increasing ϵ_a from its initial negative value, the total space charge density and hence the hydrodynamic torque decrease (see Eq. 11). The latter equation can however be satisfied by an increase in the value of a due to the presence of the flexoelectric terms.

It is interesting to note that if both the flexoelectric coefficients are decreased by a factor S, fixing the ratio $(e_1 - e_3)/(e_1 + e_3)$ at the MBBA value, a non-zero value of a is obtained only if S >0.13 (Fig. 12).

Figs.13 and 14 show V_c and a as functions of $\sigma_a/\sigma_\perp$. When the latter has a small value, the Carr-Helfrich mechanism is not very efficient and the flexoelectric terms dominate resulting in large values of a and V_c. As $\sigma_a/\sigma_\perp$ is increased, the Carr-Helfrich mechanism becomes more efficient and both a and V_c decrease initially. With further increase in $\sigma_a/\sigma_\perp$, while V_c continues to decrease, a gradually increases. The increase in $a, /\sigma_\perp$ increases the transverse electric field gradient (see Eq.4) and hence the flexoelectric torque on the director as we11 as the value of a.

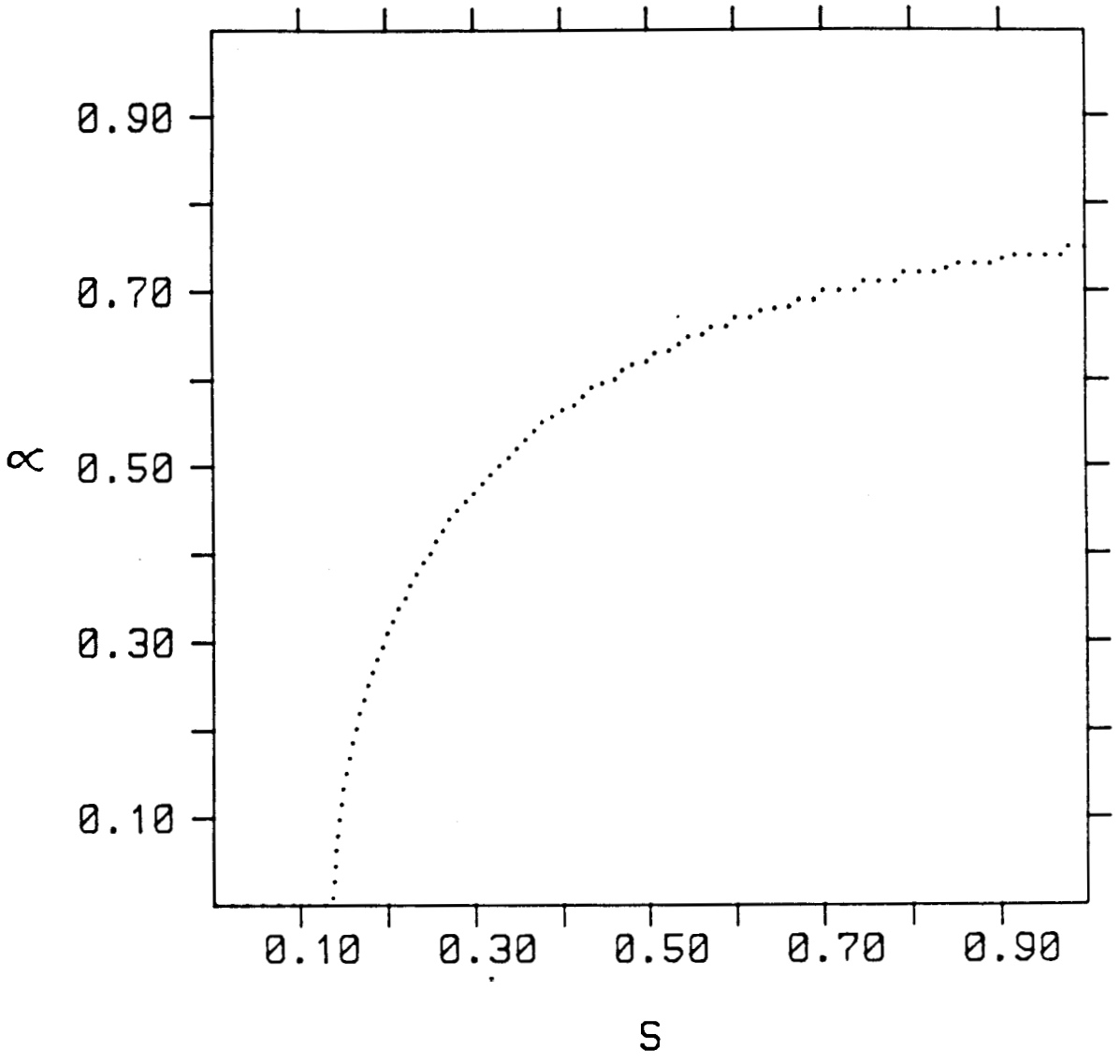

Fig.12. Variation of a (in radians) with the factor S by which the flexoelectric coefficients are decreased, keeping the ratio $(e_1 - e_3)/(e_1 + e_3)$ fixed at the MBBA value. Note that a = 0 for S < 0.13.

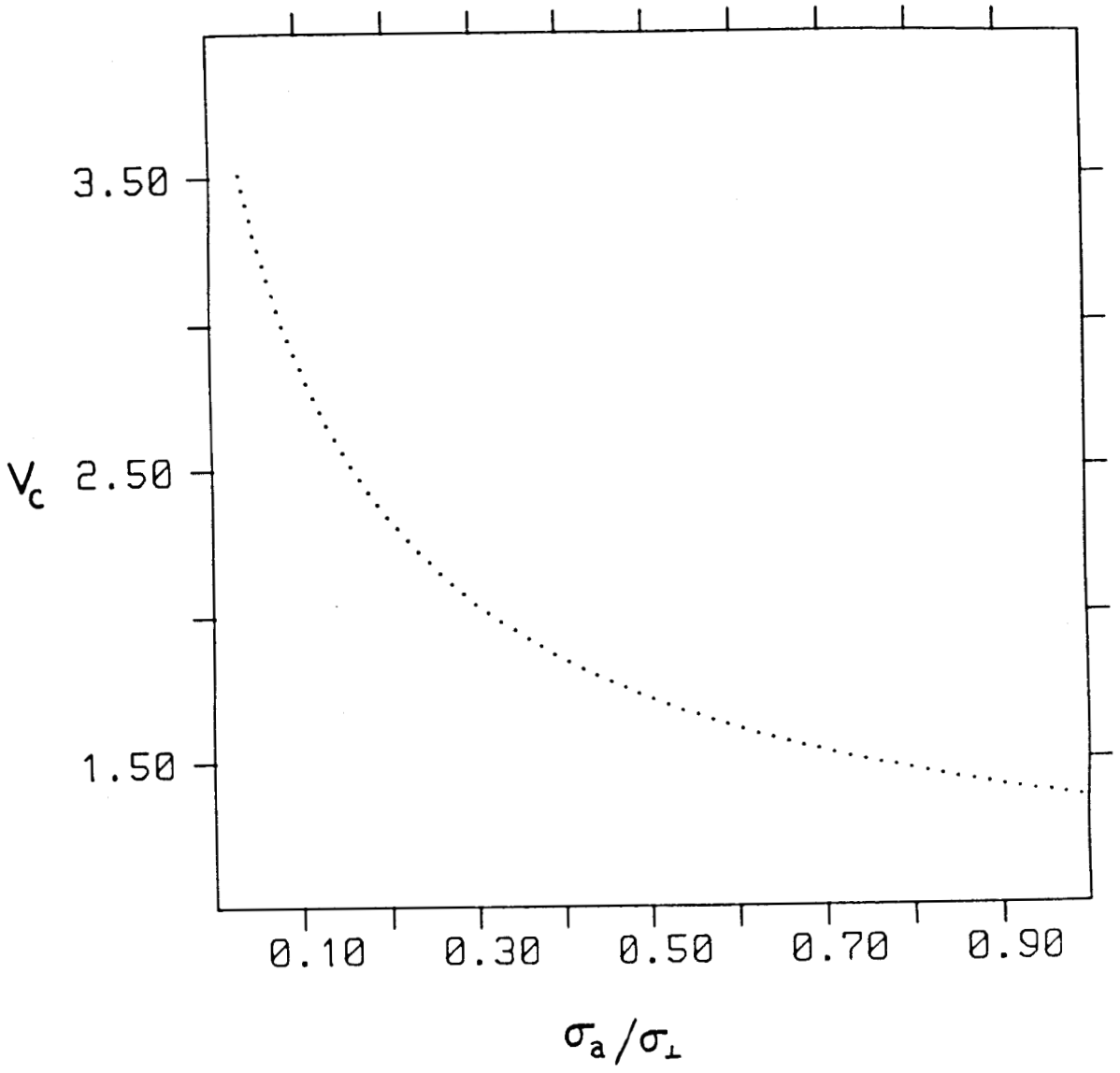

Fig.13. Variation of the critical voltage V_c (in Volts) with $\sigma_a/\sigma_\perp$.

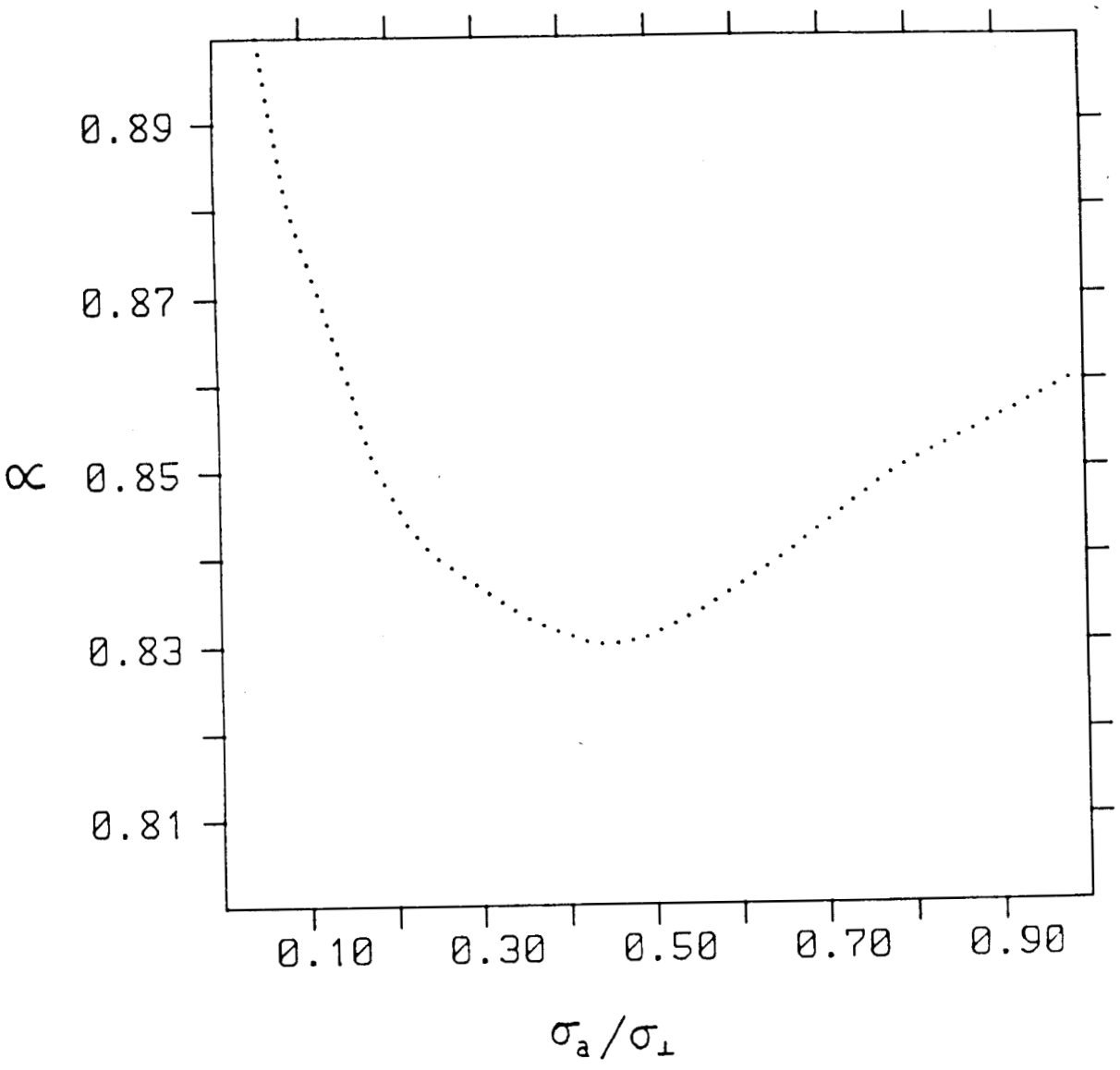

Fig.14. Variation of a (in radians) with $\sigma_a / \sigma_\perp$.

3.5 EXPERIMENTAL RESULTS

Most of the DC studies on EHD instabilities in nematics have been made on MBBA. This material is chemically unstable and the DC instability exhibited by it is known to be influenced by charge injection at the electrodes [6]. Consequently, the optical pattern observed at the onset of the instability is not the set of linear rolls expected from the Carr-Helfrich mechanism, but a complicated two dimensional pattern [6,7]. We have studied a room temperature nematic mixture containing two chemically stable compounds, viz, CE-1700 and PCH- 302 of Roche chemicals. The low frequency principal dielectric constants and the principal conductivities were measured at 1592 Hz using a Wayne Kerr bridge (B642). The values obtained at room temperature are: $\epsilon_{\parallel} = 3.3$, $\epsilon_{\perp} = 4.3$ and $\sigma_{\parallel}/\sigma_{\perp} = 1.1$. As our main objective was to study the influence of flexoelectricity on the DC EHD instability, we also measured the flexoelectric coefficients of this mixture. The experimental details are described in chapter 7. $(e_1 - e_3)/K$ and $(e_1 + e_3)/K$ were found to be about 100 and -200 cgs units, respectively. Note that these values are comparable to the MBBA values (table 1) and have the same signs.

The sample thickness was typically about 20 μm in most

of the studies. Under DC excitation the EHD instability gives rise to a set of convective rolls at the threshold (Fig. 15). Further, the instability was not observed when the thickness of the sample was less than about 5 μm. As discussed in chapter 2, the existence of a critical thickness below which the EHD instability cannot be observed is characteristic of the Carr-Helfrich mechanism. As the thickness of the sample is decreased the director relaxation time decreases becoming smaller than the charge relaxation time when the thickness is less than a critical value. Then the fluctuations in the director field do not last long enough for the formation of space charges either due to the Carr - Helfrich mechanism or the flexoelectric polarization. From the existence of a critical thickness we conclude that these mechanisms are responsible for the DC instability in the material under study and that the influence of charge injection is negligible. At the onset of the instability the wavevector of the convective rolls was found to make an angle of about 20' with the direction of the initial alignment of the director. Though the occurrence of these oblique rolls is clearly predicted by the theory presented above, a detailed comparison of the theoretical predictions with the experimental results is not possible since many of the material parameters of the mixture under study are unknown.

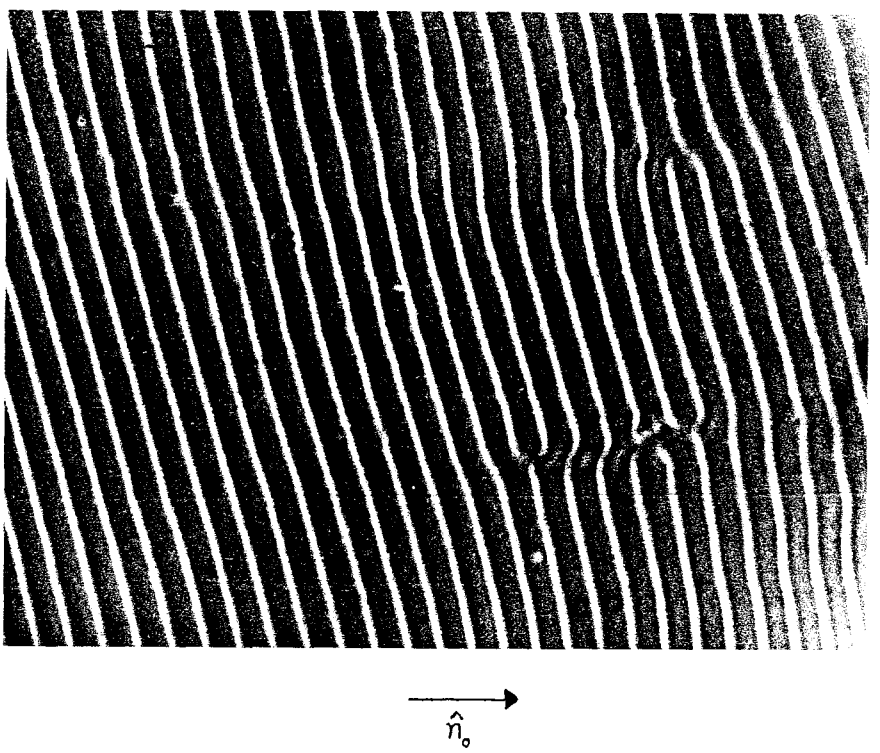

Fig. 15. Photograph of the EHD pattern obtained slightly above the threshold of the DC instability in a room temperature nematic. The orientation of the undistorted director $\mathbf{n}$ is indicated in the figure. Note that the edge dislocation in the pattern corresponds to the addition of one optical domain, which has two convective rolls of opposite vorticity as explained in the text. The sample thickness was about 15 μm. (Magnification: x 250).

We also found that the width of the optical domains is approximately twice the sample thickness. Trace'r particle motion within the domains clearly shows that each optical domain consists of two convective rolls of opposite vorticity. This is also indicated by the edge dislocation in the optical pattern, which corresponds to the termination of just one optical domain (Fig. 15). Fig.16a shows the dark fringes obtained when the sample taken between crossed polarizers was viewed through a tilting compensator, at a voltage close to the critical value. These dark bands correspond to regions in the sample where the phase difference introduced by the sample in the incident linearly polarized light is offset by the compensator. These fringes show very clearly that the effective birefringence of the sample varies more sharply at the bright lines of Fig.15 than in the region between two bright lines. When the field is increased beyond the threshold this asymmetry in the variation of the effective birefringence in the two regions becomes more pronounced (Fig.16b). These observations indicate that the director profile within the rolls is non-sinusoidal with the curvature in the region of the bright lines being much stronger than that in the region mid-way between two bright lines. The increase in the asymmetry with the field strength above the threshold shows that nonlinear terms

a

b

Fig.16. (a) The dark fringes obtained when the sample was viewed in sodium light through a tilting compensator. The applied voltage was close to the threshold value. (b) As in (a), but at a slightly higher voltage.

are responsible for the observed optical pattern. Further, when the field direction is reversed, the bright lines were found to shift by about half the optical domain width. The polarity dependence of the optical pattern suggests that flexoelectricity must be responsible for the non-sinusoidal director profile, as it is the only bulk property of a nematic that couples linearly to an external electric field. Including the second order terms and taking a = 0 for simplicity, the torque balance equation along Y is given by

$$K_3(d^2\theta/dX^2) - (e_1 + e_3)(\alpha_2/\eta) E_a\theta (d\theta/dX)$$
$$+ [\epsilon_a\sigma_\perp/(4\pi\sigma_{||}) + (\epsilon_a/\epsilon_{||} - \sigma_a/\sigma_{||})\alpha_2\epsilon_{||}/(4\pi\eta)]E_a^2\theta = 0 \qquad (14)$$

where $\eta = \frac{1}{2}(\alpha_4 + \alpha_5 - \alpha_2)$.

The lone quadratic term in the above equation arises from the action of $\vec{E}_a$ on the fleroelectric contribution to the space charge density. This equation was solved graphically by the phase plane technique using the standard MBBA values of the material parameters. The resulting non-sinusoidal θ profile and the effective birefringence are shown in Fig. 17. The variation of the effective birefringence is sharper in regions like B than in regions like A. The incident light is therefore brought to focus at two different planes by the two sets of

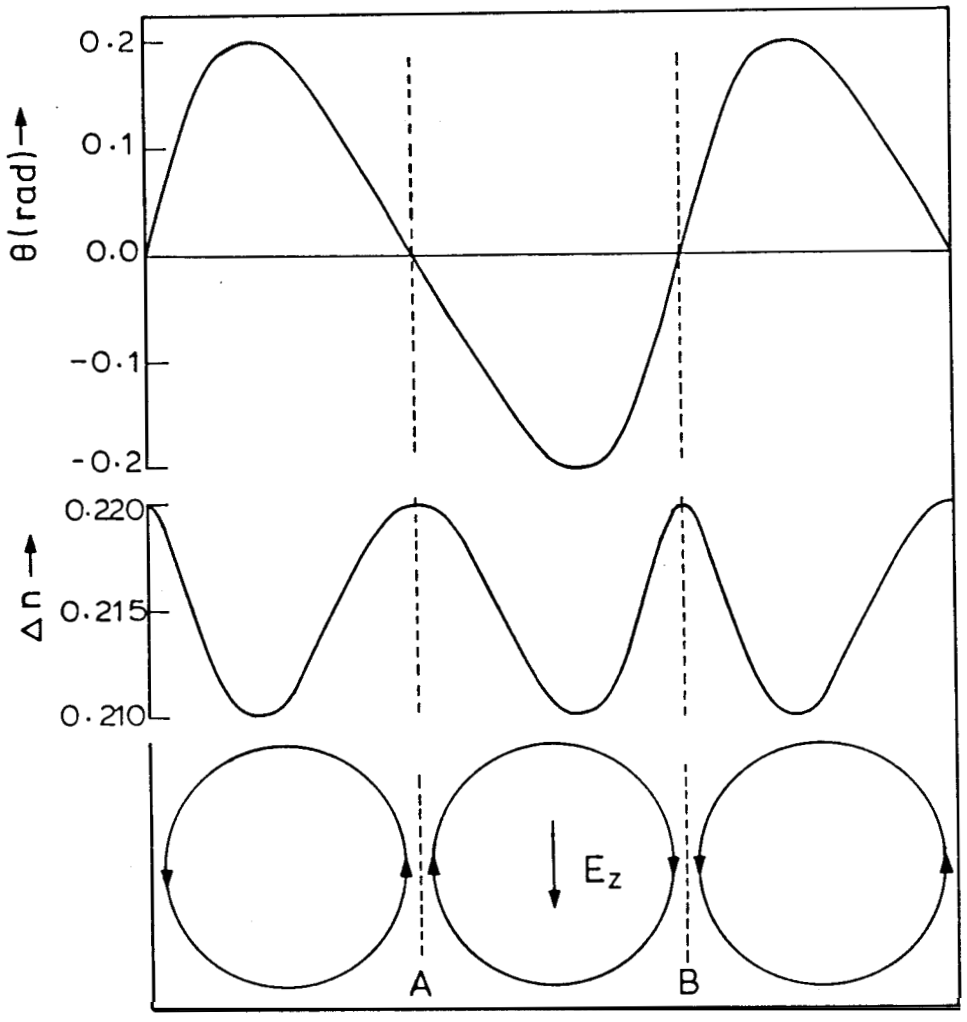

Fig.17. The non-sinusoidal director profile obtained from Eq.(14)(top). The resulting variation of the effective birefringence An with X (for n_e= 1.769, n_o = 1.549) (middle). The disposition of the convective rolls (bottom) agrees with the observed tracer particle motion, regions B corresponding to the bright lines of Fig.15.

regions. When the microscope is focussed on the set of bright lines due to regions like B, the lines corresponding to regions like A become very diffused and faint. The disposition of the convective rolls with respect to the bright lines shown in Fig.17 agrees with the observed dust particle motion. When the field is reversed, the director field in regions like A becomes more distorted than in regions like B and the bright lines shift to A, in agreement with the experimental observations.

We must note here that as discussed by Hirata and Tako [8], an asymmetry in the optical pattern will also arise from a sinusoidal director profile in the convective rolls. This is caused by the tilting of the rays due to the periodic variation of the effective extraordinary refractive index in the sample (Fig. 18). However, this weaker asymmetry does not depend on the polarity of the applied field as the director profile in the conduction regime does not oscillate with the field, and is present under an applied AC field also.

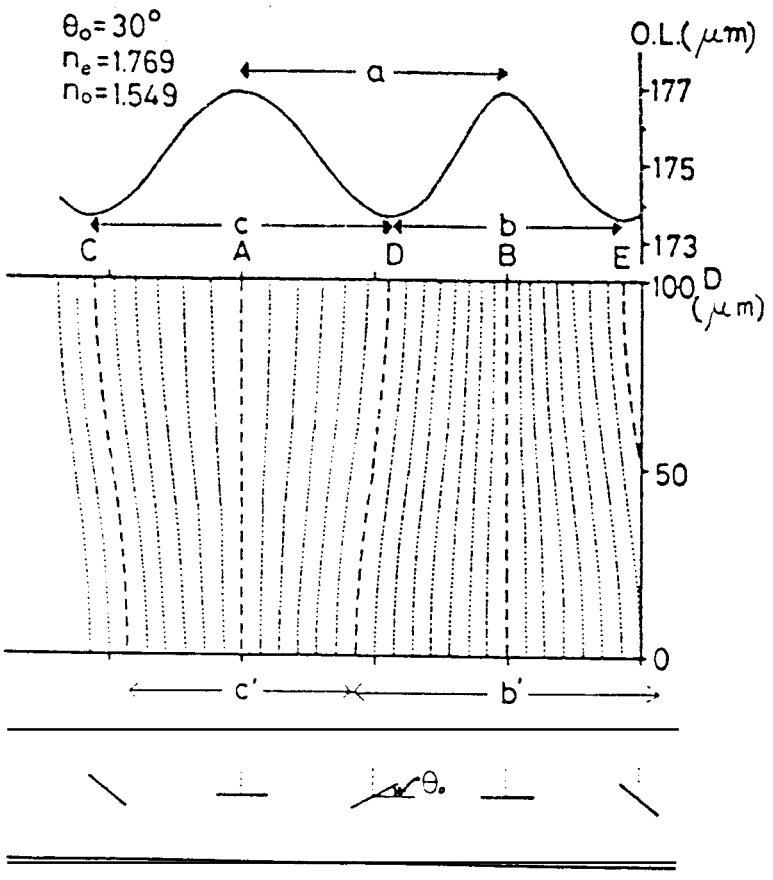

Fig.18. Ray distribution in Williams domains (dashed and dotted lines) and the corresponding optical path length (OL). The dashed lines give the rays following the shortest and longest paths. D is the cell thickness and θ_o the maximum tilt of the director.

REFERENCES

1. R.B. Meyer, Phys. Rev. Lett., 22, 918 (1969).
2. J. Prost and J.P. Marcerou, J. de Phys., 38, 315 (1977).
3. W. Helfrich, J. Chem. Phys., 51, 4092 (1969).
4. C. Fan, Mol. Cryst. Liq. Cryst., 13, 9 (1971).
5. E. Dubois - Violette, P. G. de Gennes and O. Parodi, J. de Phys., 32, 305 (1971).
6. Orsay liquid crystal group, Mol. Cryst. Liq. Cryst., 12, 251 (1971).
7. S. Hirata and T. Tako, Jpn. J. Appl. Phys., 20, L459 (1981).
8. S. Hirata and T. Tako, Jpn. J. Appl. Phys., 21, 675 (1982).